G. Le Besnerais, F. Champagnat,
A. Plyer, R. Fezzani,
B. Leclaire, Y. Le Sant
(Onera)

E-mail:
guy.le_besnerais@onera.fr

Advanced Processing Methods for Image-Based Displacement Field Measurement

We present recent developments in data processing for velocity field estimation and visualization originating from computer vision. We review the current paradigm of PIV data processing, based on window correlation, and the regularization or variational approach which is dominant in optical flow estimation. We propose a novel unifying framework via the optimization of a compound regularized criterion written in terms of a dense displacement (or velocity) field. The paper then focuses on algorithmic issues. A fast iterative window correlation method leading to a highly parallel algorithm termed FOLKI is described. Thanks to a GPU (Graphical Processing Unit) implementation, FOLKI reaches video rate for typical PIV data. Then we present more sophisticated solvers able to deal with the regularization term of the criterion, notably multigrid methods.
In our view, these two components form the foundation of a video rate velocity field visualization and interpretation toolbox which, together with recent advances in experimental apparatus and numerical simulation, opens the way to a major development in experimental fluid science.

Introduction

Photometry and photogrammetry are the two main image-based methods for measuring physical quantities. In photometry, the parameter investigated is a function of the intensity level: an example is the measurement of pressure on the surface of an object in a wind tunnel by means of Pressure Sensitive Paint (PSP). In photogrammetry, we are interested in the shape of some image patterns or in their apparent motion from one image to the other so as to measure geometric quantities such as distance, velocity, strain, etc.; classical examples are Model Deformation Measurement (MDM) and Particle Image Velocimetry (PIV) (see the other contributions on these techniques in this issue).

This paper looks at photogrammetry, and focuses on the measurement (or estimation) of displacement fields from image sequences. Estimation problems like these occur in the experimental study of fluid dynamics via dedicated imaging techniques such as Laser Tomoscopy and PIV and also in experimental characterization of strain on solids. These techniques, which are related to the domain of image motion or optical flow estimation in computer vision, are the subject of Onera's research project MEMFIS which associates computer vision specialists with physicists from fluid mechanics and materials science.

Following on seminal work dating back from the 80's [1, 2], motion estimation in computer vision is now rapidly developing again under three main driving forces: (i) the renewal of the methodological framework – notably physically sound regularization models tailored for fluid dynamic, see § "Regularisation framework for displacement field estimation"; (ii) assimilation of the applied mathematics corpus into the estimation algorithm (i.e. multi-grid methods [3], sub-domain decomposition, etc.); (iii) technological advances in generic computing hardware, notably the development of one-chip massively parallel architectures, such as multi-core CPUs and GPUs.

These recent developments are still widely ignored in the PIV community. This paper is one of a series of recent initiatives that the computer vision community has taken in the field of PIV [4, 5]. Contrarily to most of these works it emphasizes the points (ii) and (iii), i.e. algorithm and architecture for fast computation of the displacement field. Indeed, we believe that computational efficiency is the key to the spread of methodological advances on fluid displacement estimation and interpretation within the PIV community, for two main reasons:

1. advances in experimental PIV (Time Resolved PIV, 3D tomographic PIV) yield a huge data flow to be processed;
2. advanced processing methods usually come up with more tuning parameters, whose influence is often more difficult to predict, so their use requires a high level of interaction with the user.

The rest of the paper is divided in three parts: the firt one formulates displacement field estimation within a general regularization framework and presents the main algorithmic issues, the second one focuses on fast window-based estimation algorithms, then we briefly presents algorithmic trends for solving the large non linear systems yielded by regularized approaches. To conclude remarks and prospects are gathered together.

A regularization framework for displacement field estimation

PIV and interrogation windows

Fundamentally, in PIV or in other fields where image velocity is required, such as video coding or optical flow estimation in computer vision, the problem at hand is to estimate a displacement field $d(x)$ from two images $I(x, t_1)$ and $I(x, t_2)$ – velocity is derived from the time interval $t_2 - t_1$ between images. At this point, most authors in PIV introduce the notion of an "interrogation window" (IW), i.e. a square area containing a certain number of particles (say 10) that form some random pattern that can be detected and localized in the next image. This search leads to a displacement vector which is attributed to the center of the interrogation window. The size of the interrogation window is the main parameter of this approach: it defines the resolution of the result, i.e. the spatial sampling of the estimated displacement fields (typically half the IW size). Moreover, the window size tunes the "bias versus variance" trade-off of the estimation process. Larger windows lead to smoother estimated fields. The variance of the estimation error is lowered but so are small-scale motions, which means a bias toward the constant displacement field. There are of course several developments in modern PIV software that improve on this trade-off: image preprocessing, iterative window refinement, vector field post-processing, etc. The concept of an interrogation window still influences and, as we will try to demonstrate here, essentially limits the development of innovative PIV processing.

Modern optical flow and regularization

Modern optical flow estimation starts from a more abstract problem: if $I(x,t)$ is the image intensity at position x and time t and assuming that the recorded images correspond to time instants t_1 and t_2, the problem can be expressed as the search for a displacement field $d(x)$ which satisfies the so-called image registration condition

$$I(x,t_1) = I(x + d(x), t_2), \quad \forall x \tag{1}$$

In practice, this condition is relaxed by searching the peak of the cross-correlation or by minimizing the least-square criterion

$$\sum_x \left(I(x,t_1) - I(x + d(x), t_2) \right)^2 \tag{1b}$$

see box 1. This image registration problem is in general indeterminate: very different and often "non-physical" displacement fields lead to a low criterion. Indeterminacy stems from two facts: (i) being a scalar equation of a 2D unknown vector, the registration condition clearly yields less than half the number of equations that would be necessary; (ii) moreover, the recorded images are blurred, noisy and sampled versions of the image intensity, which means that only an approximation of the registration criterion (1b) is computable.

Box 1 - Optical flow and optical flow

The term "optical flow" has various meanings depending on the domain and context. In the PIV community, optical flow is often associated with the work of Quénot et al. [25]. This is an unfortunate confusion, because [25] describes a particular technique based on window correlation and dynamic programming, two elements which depart notably from the vast majority of optical flow estimation methods in computer vision. A much more "main-stream" application of optical flow to PIV can be found in [4].

Optical flow is also often associated with a first order expansion of the registration condition (1) for small motion d and time interval $dt = t_2 - t_1$:

$$\frac{\partial I}{\partial t} + (\nabla I)^t \, d = 0 \tag{I.1}$$

This so-called "optical flow constraint" (OFC) is central to historical references on optical flow such as the work of K.B. Horn and B. Schunck [1], and is still used in several recent references such as [10]. However, OFC is valid only for very small displacements and since the end of the 90's, many authors have proposed that the more general condition (1) should be considered to deal with large displacements. The expression "modern optical flow" which is used in the text refers to this large displacement context which is, in our opinion, the right framework for PIV processing.

Let us emphasize that the main difference between (I.1) and (1) is that the latter is non linear with respect to the displacement field. To deal with the non linearity, the estimated field is iteratively refined, by means of a first order development of (1) around a previous estimate d_0. Writing $d = d_0 + \delta d$, the flow increment satisfies a first-order condition which is similar to the OFC constraint:

$$I(x + d_0(x), t_2) - I(x, t_1) + (\nabla I(x + d_0(x), t_2))^t \, \delta d = 0 \tag{I.2}$$

Hence classical optical flow approaches based on the OFC often appear inside the iterative process of modern "large displacement" optical flow estimation.

Finally, we should discuss implementation issues, related to the fact that the images are recorded on a square grid of pixels positions. Assuming, without loss of generality, that the sampling step is 1, equation (I.2) is written for discrete positions m, associated with pixels of image $I(m, t_1)$. However, (I.2) also includes values of image $I(m, t_2)$ for real positions such as $m + d_0(m)$ which are shifted by the initial displacement field d_0. The resulting image $m \rightarrow I(m + d_0(m), t_2)$ is a warped version of $I(m, t_2)$. In image processing, warping an image $I(m, t_2)$ consists in interpolating its values on real warped positions by means of a spatial interpolation, using for instance a kernel-based interpolation such as

$$\tilde{I}(x,t) = \sum_m \gamma(x - m) I(m,t) \tag{I.3}$$

This interpolated image is also used to define the spatial gradient values required in (I.2).

The classical answer to such ill-posed problems is regularization [6]. It consists of complementing the data with prior information on the investigated object, here the displacement field. In the line of the works of Philips-Twomey-Thykonov in the 60-70's (see references in Chapter 1-2 in [6]), this information is often expressed as a constraint on some derivative functional of the displacement field $f(d)$. For optical flow estimation, a popular choice is the Horn and Schunck regularizing functional [1]:

$$f(d) = \|\nabla d_u\|^2 + \|\nabla d_v\|^2, \quad for \quad d = [d_u, d_v] \tag{2}$$

The estimated displacement field is then defined as the minimizer of a regularized criterion such as:

$$J(d) = \int \psi\left((I(x,t_1) - I(x+d(x),t_2))^2\right)dx + \lambda \int \Phi\left(f(d)\right)dx \tag{3}$$

where ψ and Φ are potential functions, and λ is the regularization parameter. The simplest choice is the quadratic penalization, associated to trivial potentials $\psi(s^2) = \Phi(s^2) = s^2$. Such approaches are often termed "variational optical flow estimation" in recent papers such as [4, 7]

Qualitative comparison on a real PIV dataset

Box 2 presents a comparison of estimated displacement fields on the central (512 x 512) part of images 25-26 of the PIV Package3 dataset of the European interdisciplinary FLUID project [5]. This package is made of experimental PIV images of a slightly turbulent air flow seeded with small water droplets: see one frame in figure B2 - 01.
The left part of figure B2 - 02 shows the estimated displacement field using a window-based method. It is derived from the dense window-based algorithm FOLKI, which is the topic of Section 3. Except for the density of the estimated field (one vector per pixel), this result is a typical output of current PIV software. On the right is the result of the minimization of regularized criterion (3) with regularizing functional (2). In other words, this variational optical flow estimate does not use any interrogation window; the goodness-to-fit term is simply a pixel-wise registration criterion. As can be seen, despite their very different rationales both approaches give similar results with this example.
Finally, figure B2 - 03 presents several results for varying parameters. The four fields on the top line are estimated using the window-based method with a Gaussian weight function of standard deviation 4, 6, 12 and 26 from left to right. The four fields on the bottom line are derived from the minimization of (3) with regularizing functional (2) and four different choices of the regularization parameter ($\lambda =$ 100, 1000, 1.10^4, 3.10^4, from left to right). Except for the two estimates on the left, which exhibit large errors, all other reconstructions appear correct. Looking at the various degrees of smoothness of the estimates, it should be clear to the reader that the regularization parameter in (3) plays a role similar to the window size in the aforementioned "bias vs. variance" trade-off: the higher λ, the smoother the solution.
The window-based approach then appears as a form of spatial regularization, which assumes that the motion field is constant at the scale of the interrogation window. As always, this regularization principle is only approximately true – actually it is absolutely wrong near regions of high velocity gradient, such as a vortex center or other discontinuities. Note, however, that the Horn and Schunck functional (2) is not particularly well suited to fluid dynamics: it has been noted, for instance in [8], that it leads to underestimation of the velocity near a vortex.

A unifying framework

As already noted by [4], the real advantage of the optical flow approach is its versatility. Contrarily to window-based approaches which all rely on the same regularization principle, modern optical flow techniques use various regularizing functionals f and various potentials ψ and Φ, which opens the way to completely different estimators [7] and in particular to techniques tailored for the particular situations of fluid dynamics [8,9,10,22,24].
In our view, regularization appears here as the expected interface between experimental and numerical studies, because choosing the right regularization tool is essentially a matter of modeling the phenomenon being studied. However, we will not discuss further the design of such regularization tools, and turn toward the essential problem of the computing the estimates. In order to do so, let us introduce a generalized version of (3), where the registration criterion includes a local window. Defining the weighted average of squared intensity differences

$$D(d,x) = \int w_\rho(x-y)\left(I(y,t_1) - I(y+d,t_2)\right)^2 dy, \quad \forall (x,d) \tag{4}$$

using the normalized and separable (i.e. isotropic) Gaussian kernel w_ρ of standard deviation ρ, this unifying regularized criterion is written:

$$J(d(\cdot)) = \int \psi\left(D(d(x),x)\right)dx + \lambda \int \varphi\left(f(d;I)\right)dx \tag{5}$$

Convolution of the squared intensity difference with a Gaussian kernel introduces a spatial integration of the registration criterion over the essential support of w_ρ. Such a criterion is a generalization of the CLG approach of Bruhn *et al*. [3] to the large displacement context. It unifies a window-based approach (ρ typically around 16 pixels and $\lambda = 0$) and a regularized criterion like (3) ($\rho \to 0$ and $\lambda > 0$). Note also that the regularization functional f in (5) depends on the image intensity I: indeed, some authors use the local image gradient to tune the regularization (it is called "image driven regularization" in [7]).

In the sequel we focus on numerical methods for fast optimization of criterion J of (5) with respect to the dense vector field d for various values of ρ and λ. Next section will discuss the optimization in the case $\lambda = 0$, and the final part of the article will discuss current approaches for the general case.

Window-based estimation of dense velocity fields at video rate

Introduction

In this section, we consider the optimization of (5) for $\lambda = 0$. As there is no longer a regularization term in this case, the optimization boils down to a separable problem where each vector of the field is sought in order to minimize a local registration criterion, spatially integrated on a local window whose extension is given by the shape of the weight function w_ρ. This approach belongs to the paradigm of window-based methods that underlies commercial PIV software and has been reviewed in previously. The main difference lies in the optimization process. The proposed iterative process, described in the following section and box 3, allows for fast computation of a dense field, whereas FFT-based PIV software yields under sampled vector fields, typically by a factor of 16 on each dimension (considering for instance an interrogation window size of 32*32 pixels with 50% overlap between adjacent windows, which can be a standard setting in PIV campaigns).

Box 2 - Estimation with window-based and variational methods on real PIV data

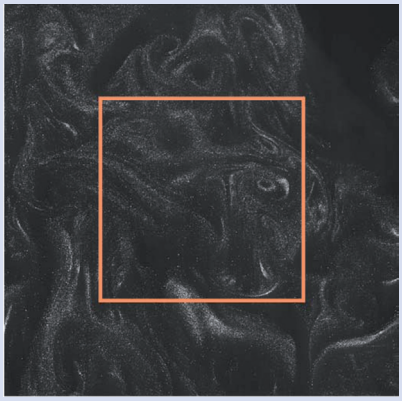

Figure B2 - 01. One image of the dataset “Package3” from the FLUID project [5]: experimental PIV on a slightly turbulent air flow seeded with small water droplets. Only the central part (512 x 512 orange square) of the motion field has been computed in the sequel.

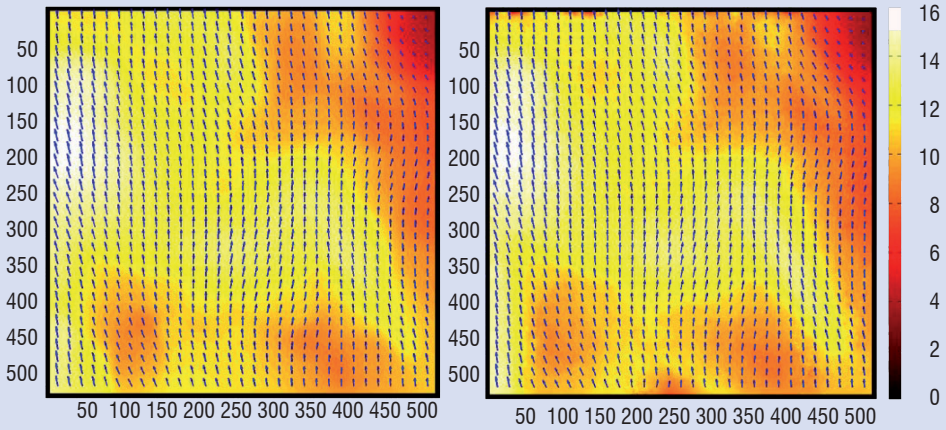

Figure B2 - 02. Results of displacement field estimation for two images of the dataset “Package3” from the FLUID project [5]. Norm of the field in color (see color map) Left: window-based dense approach (algorithm FOLKI, see Section 3) with a Gaussian window of standard deviation 12. Right: variational approach, estimation obtained by minimization of criterion (3) with Horn and Schunck’s regularizing functional (2) and a regularization parameter $\lambda = 1000$. Note the similarity between both methods, despite their different rationale.

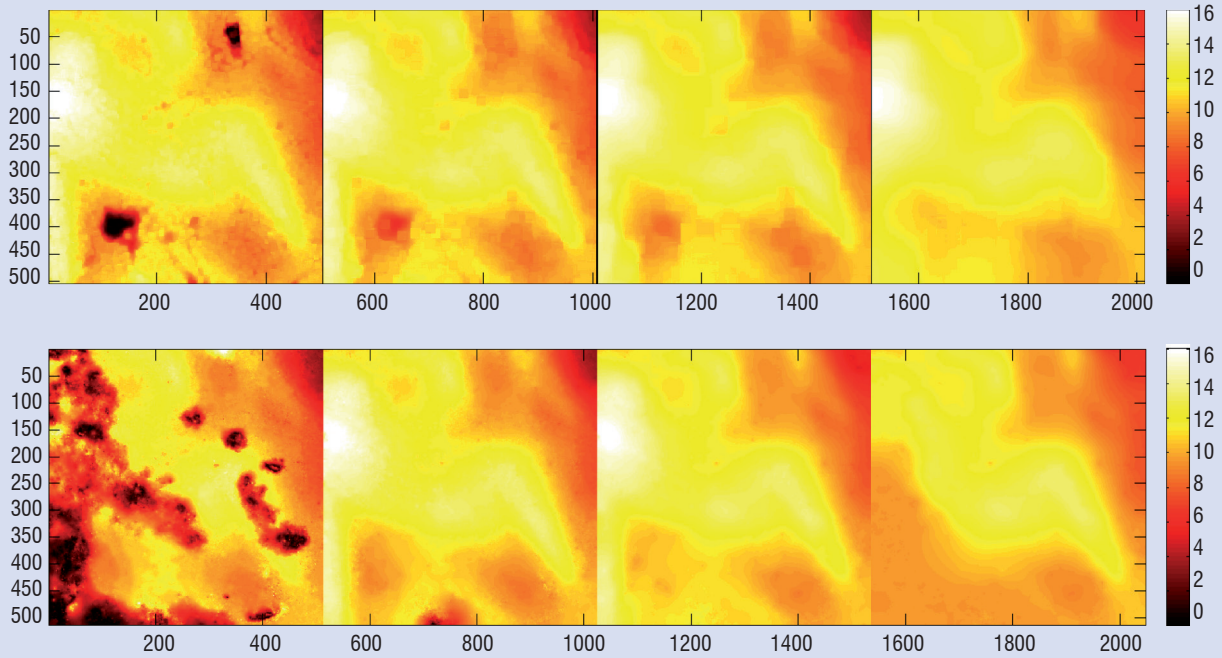

Figure B2 - 03 - Results of displacement field estimation for two images of the dataset “Package3” from the FLUID project [FLUID]. Top: norm of the optical flow estimated using a window-based dense approach with a Gaussian window of standard deviation 4, 8, 16 and 32 (from left to right). Bottom: norm of the estimate obtained by minimization of the regularized criterion (3) with regularizing functional (2), regularization parameter set to 100, 1000, 1.10^4, 3.10^4 (from left to right). The degrees of smoothness of the result can be controlled in both methods, either by the window radius (i.e. standard deviation of the Gaussian) or the regularization parameter.

Box 3 - Iterative window registration

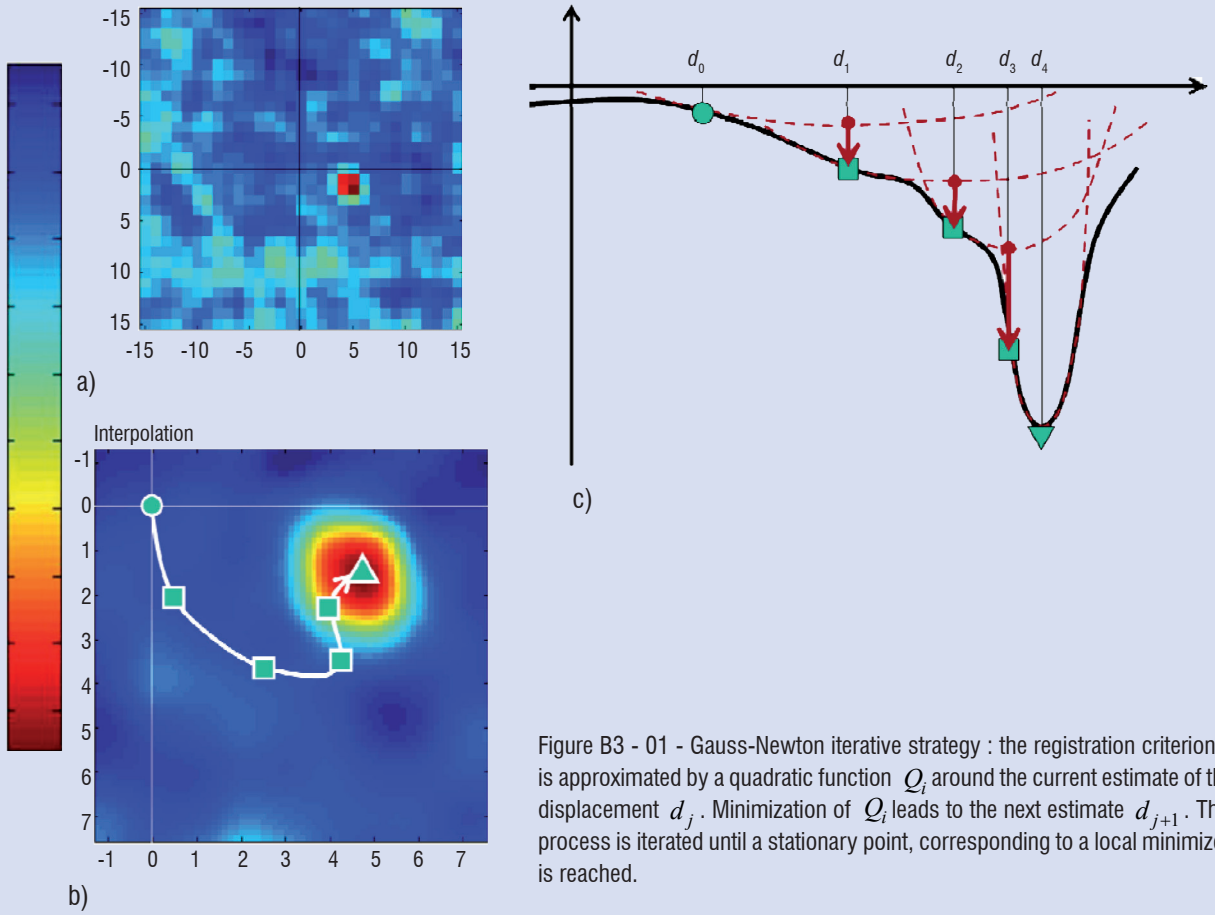

Figure B3 - 01 - Gauss-Newton iterative strategy : the registration criterion A is approximated by a quadratic function Q_i around the current estimate of the displacement d_j. Minimization of Q_i leads to the next estimate d_{j+1}. This process is iterated until a stationary point, corresponding to a local minimizer, is reached.

The cross-correlation function $R(d)$ associated with the search of an interrogation window W from image $I(x,t_1)$ to image $I(x,t_2)$ was defined in [21, box 1]. It is usually computed all over a grid of possible displacements d so as to find a maximum. Here, we use a quadratic distance between interrogation window intensities (sometimes weighted by a window profile w):

$$A(d) = \sum_m w(m-k)\left(I(m,t_1) - \tilde{I}(m+d,t_2)\right)^2 = E_{t1}^2 - 2R(d) + E_{t2}^2(d) \qquad \text{(III-1)}$$

An example of registration criterion A is represented in Figure B3 - 01 - a for integer displacements d. In general, the energy of the image integrated on a window is approximately stationary and A varies as the opposite of the cross-correlation function R.
In this work, we first consider all possible real-valued displacements d: The registration criterion A is then written in terms of an interpolated image defined in Box 1, equation (I.3). Figure B3 - 01 - b shows that the criterion A appears as a smooth surface, whose maximum is sought using an iterative optimization algorithm. The Gauss-Newton iterative scheme, sketched in Figure B3 - 01 - c in the 1D case, is derived from a first order development of the residuals appearing in (III-1) in $d = d_0 + \delta d$. Around d_0, the criterion is approximated by a quadratic function

$$Q_0(\delta d) = \sum_m w(m-k)\left(I(m,t_2) - \tilde{I}(m+d_0,t_1) - \nabla\tilde{I}(m-d_0,t_2)^{\mathrm{t}}\delta d\right)^2 \qquad \text{(III-3)}$$

whose minimization yields the new estimated displacement d_1. It is interesting to derive another form of Q_0:

$$Q_0(\delta d) = [\delta d^{\mathrm{t}} \quad 1]\, H_0 \begin{bmatrix}\delta d \\ 1\end{bmatrix}, H_0 = \sum_m w(m-k)q(m)q^{\mathrm{t}}(m), \quad q(m) = \begin{bmatrix} -\nabla\tilde{I}(m+d_0,t_2) \\ I_t(m,t_1) - \tilde{I}(m+d_0,t_2)\end{bmatrix} \qquad \text{(III-4)}$$

From (III-4) it is clear that the Hessian matrix H_0 only depends on spatio-temporal derivatives of the image intensity integrated on the chosen window support.

Local search by iterative optimization

As detailed in Box 3, the search for the matching window is considered to be the iterative optimization of a nonlinear least squares registration criterion. The usual Gauss-Newton iterative optimization process relies on successive local quadratic approximations of the criterion. Since its introduction into computer vision by Lucas and Kanade [2], numerous contributions have concerned improvements of this scheme. The most significant development is conducting the search in a multi-resolution framework. These iterative and multi-resolution techniques are capable of fast window registration with a good accuracy, typically less than the tenth of a pixel, even when the true displacement is large, for instance equal to the window size [11].

Parallel Implementation for dense estimation

The previous iterative approach provides 2C velocity fields whose quality is similar to that obtained with classical FFT-based cross-correlation peak detection techniques. But the true advantage of such approaches is their highly parallel structure, when combined with dense estimates. Let us apply the Gauss-Newton strategy simultaneously to all local registration criteria whose sum forms the global criterion J of (5) with $\lambda = 0$. This global iterative scheme uses an approximate quadratic criterion which is the sum over all pixels of the quadratic forms given by (III-3 and III-4) in Box 3. Updating the whole field simply amounts to solving NxN independent 2 x 2 systems each one with a Hessian matrix given by in (III-4). A remarkable result is that in a dense framework, the coefficients of all these systems can be computed simultaneously by 2D linear filtering of the images; essentially differentiation on the pixel scale and integration on the window scale, as shown by the form of the Hessian matrixes in (III-4) of Box 3. This result has been known for years in the case of an initial null displacement, and has been generalized to further iterations in a recent paper [12]. This yields an algorithm christened FOLKI (for *Flot Optique Lucas-Kanade Iteratif*), which, on a conventional architecture, can compute a dense field for a computational cost equivalent to the computation of a 16 times under sampled field with the classical FFT-based cross-correlation.

The structure of FOLKI is ideally suited to massively parallel architectures like GPUs (*Graphics Processing Unit*). Boosted by the video games market, graphic units have become cheap, ubiquitous and powerful parallel co-processors. FOLKI has been implemented on a GPU this year [20], leading to performances unchallenged by previous techniques: the processing of a 1000 x 1400 pixel PIV image pair requires less than 30ms. This performance means that a typical PIV data set (1000 PIV pairs, each 2000 x 2000 pixel) can be processed in a few minutes. One interesting result is that the computational gain of FOLKI-GPU compared to an implementation on a classical CPU architecture increases with the image size. Table 1 below shows the computing time per-pixel on FOLKI for increasing image sizes. FOLKI-GPU yields a gain of a factor 10 for small (512 x 512) images but the factor reaches 100 for large (4096 x 2048) images. More informations on the FOLKI-GPU algorithm, including a downloadable open source software (under L-GPL license), can be found on the website www.onera.fr/dtim/gpu-for-image, which is dedicated to image and vision applications of GPU computing.
These unchallenged performances open the way to on-the-fly PIV processing inside fluid flow visualization and interpretation software. A video of the results obtained in real-time with FOLKI on dataset "Package3" from the FLUID project [5] is provided on the previously mentioned website.

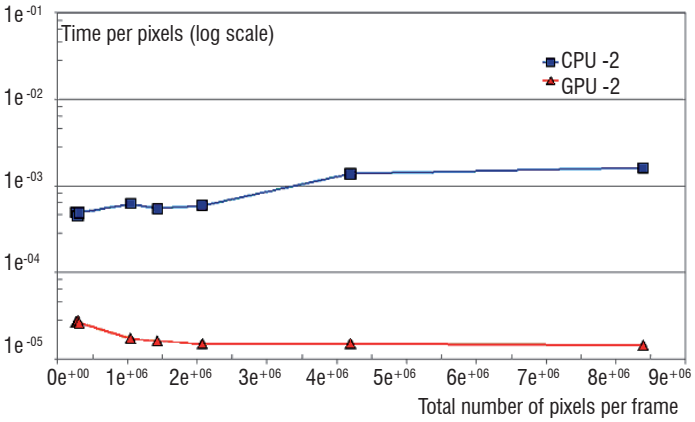

Figure 1 - Computing time per-pixel of FOLKI for increasing size of images. Comparison between computing time on a classical CPU architecture and on a GPU architecture.

Extension to Stereo PIV

The regularization framework presented before also provides a direct formulation of the Stereo PIV problem [13][14]. Stereo PIV uses the simultaneous acquisition of "left" and "right" PIV images in a stereoscopic setting to recover the out-of-plane velocity component. The classical technique consists of separately estimating velocities in each image plane (using one of the previously described techniques), then combining these two 2C estimates to estimate the 3C velocity V. We have recently proposed a direct formulation of the estimation of V [15]. This formulation introduces a nonlinear least squares criterion that cumulates the registration errors associated with left and right images. The resulting criterion is a simple generalization of J in (5) (with $\lambda = 0$) which involves the four PIV image intensities, the 3C velocity V, and projection matrices for left and right cameras derived from the geometric calibration of the system. Such a direct formulation is interesting because it makes use of the epipolar geometry during the correlation step to constrain the search domain and remove potential ambiguities. Moreover, the overall Gauss-Newton iterative multi-resolution scheme introduced for 2C estimation is entirely transferable to 3C estimation.

Toward fast global regularized estimation

Introduction

We now consider the problem of the optimization of (5) in the general case where $\lambda > 0$. Because of the regularizing functional f, typically made of spatial derivatives of the displacement field, the problem is no longer separable. In other words, in an iterative optimization scheme, based on successive linearization of the registration term following equation I-2 in Box 1, the system which has to be solved at each iteration is no longer diagonal (or 2x2 block diagonal, like the one in § "Local search by iterative optimization") but involves a $2N$x$2N$ matrix. In general the optimization of such a non linear coupled criterion of around 2 million variables would be a formidable, if not intractable, task. Two elements simplify the problem: (i) the non linearity of the registration term can be dealt with in a multi-resolution framework, see next section and Box 4; (ii) inside an iteration of the algorithm, efficient multigrid solvers can be used thanks to the structure of the linearized problem.

Multi-resolution estimation

Multi-resolution estimation is closely linked to the theory of scale-space in computer vision and image analysis [16]. It consists in associating with an image a one-parameter family of smoothed images (the "scale-space representation") parameterized by the size of the smoothing kernel used for suppressing fine-scale structures. The most popular smoothing kernel is the 2D separable Gaussian kernel $g_\sigma(x)$, which is parameterized by its standard deviation σ. The resulting representation can be written as $I(x;\sigma) = (g_\sigma * I)(x)$.
As the spectral content of $I(x, \sigma = 2)$ is halved in both directions with respect to the original image, it can be represented with sampling periods twice the original ones, i.e. using $N/2 \mathrm{x} N/2$ coefficients if the original image was discretized on $N \mathrm{x} N$ pixels. We then get a pyramid of images $\{I^{(j)}(x)\}$ by setting $I^{(0)}(x) = I(x)$ and recursively convolving by g_2 and down-sampling the previous image, the level j image $I^{(j)}$ being discretized on $N/2^j \mathrm{x} N/2^j$ pixels if the original ones was $N \mathrm{x} N$. A discrete version of this so-called Gaussian pyramid has been proposed in 1983 by Burt and Adelson [17], an example on a PIV image is presented in Box 4.
The rationale for such a redundant representation is the fact that several phenomena of interest in image and video analysis (edges, segments, motions, etc.) have a characteristic scale. Analyzing the image at this particular scale, by using the corresponding image in the chosen scale-space representation, gives better detection of the phenomenon. For instance, in motion estimation, large displacements are usually easier to estimate on coarse scale images. From a theoretical point of view, Lefébure and Cohen showed that the registration of coarse-scale images yields a criterion "more convex" than the registration of the original fine scale images [18]. The multi-resolution estimation scheme then consists in a coarse-to-fine refinement of the estimated motion. Using for instance the Burt-Adelson Gaussian pyramid, we initialize the estimated displacement by the null field at level J, registers $I^{(j-1)}(x,t_1)$ and $I^{(j-1)}(x,t_2)$ estimate a first displacement field $d^{(J)}$. Transition to the next finer scale consists in up-sampling and magnifying the estimated field by a factor 2 to initialize the registration of $I^{(j-1)}(x,t_1)$ and $I^{(j-1)}(x,t_2)$ – usually this initialization is done by warping one of the images (the warping operation is explained in box 1, Eq. (I.3)). This process is reiterated until the original $(j = 0)$ resolution level is reached.
An example of multi-resolution estimation is given in box 4. Figure B4 - 01 compares the displacement field obtained with a multi-resolution process on the left to the one obtained with multiple iterations at the original resolution level on the right. The latter field is presented with a scale factor of 50 on the vectors, which are largely under estimated and appear trapped in several local minima of the registration criterion. The multi-resolution process avoids these minima and yields a correct flow. Note that recently Ruhnau et al. [4] have proposed a true multi-scale estimation process, using not only the reduced images of the Gaussian pyramid, but also intermediate smoothed images $I(x,\sigma)$. According to this reference, this approach is particularly beneficial for PIV image processing, because PIV images are usually very spiky and, even using a multi-resolution scheme, one could be trapped in a local minimum.

Box 4 - Multi-resolution coarse-to-fine scheme

We present experimental evidence about the benefits of a coarse-to-fine multi-resolution scheme for estimating displacement fields in PIV. We first compare the results obtained with a multi-resolution scheme and those obtained with iteration at level 0, i.e. by working directly on the original image resolution. As can be seen in the right part of Figure B4 - 01, the latter strategy leads each vector to the closest local minimizer.

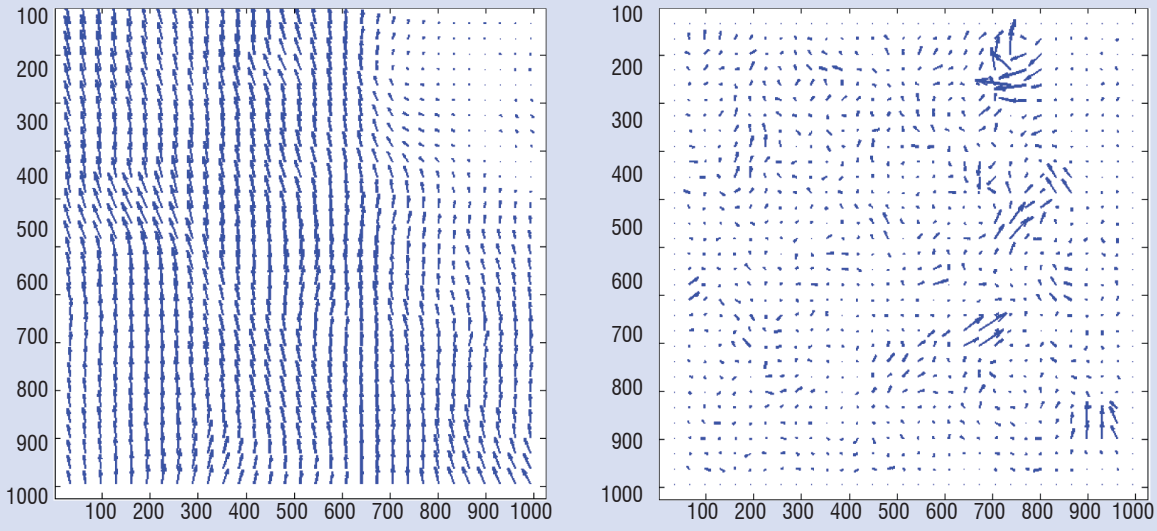

Figure B4 - 01 - Comparison of estimated displacement fields with the FOLKI window-based algorithm (Gaussian weight function with standard deviation 12) on 2 images of the dataset "Package3" from the FLUID project [5]. Left: result of a multi-resolution scheme, 3 resolution levels, 2 iterations on each level, vectors magnified by a factor of 2; right: result of 4 iterations at level 0, vectors magnified by a factor of 50.

Then we present intermediate results (only their norm is shown) for three levels of a multi-resolution coarse-to-fine strategy, in front of the corresponding sub-sampled image. The main motions are already correctly estimated on the level 3 (128 x 128) result. At this scale, the maximum displacement is 2 pixels. This estimate is up-sampled and multiplied by a factor of 2 and then refined at resolution level 2, while descending the resolution pyramid until the original scale (not shown here) is reached.

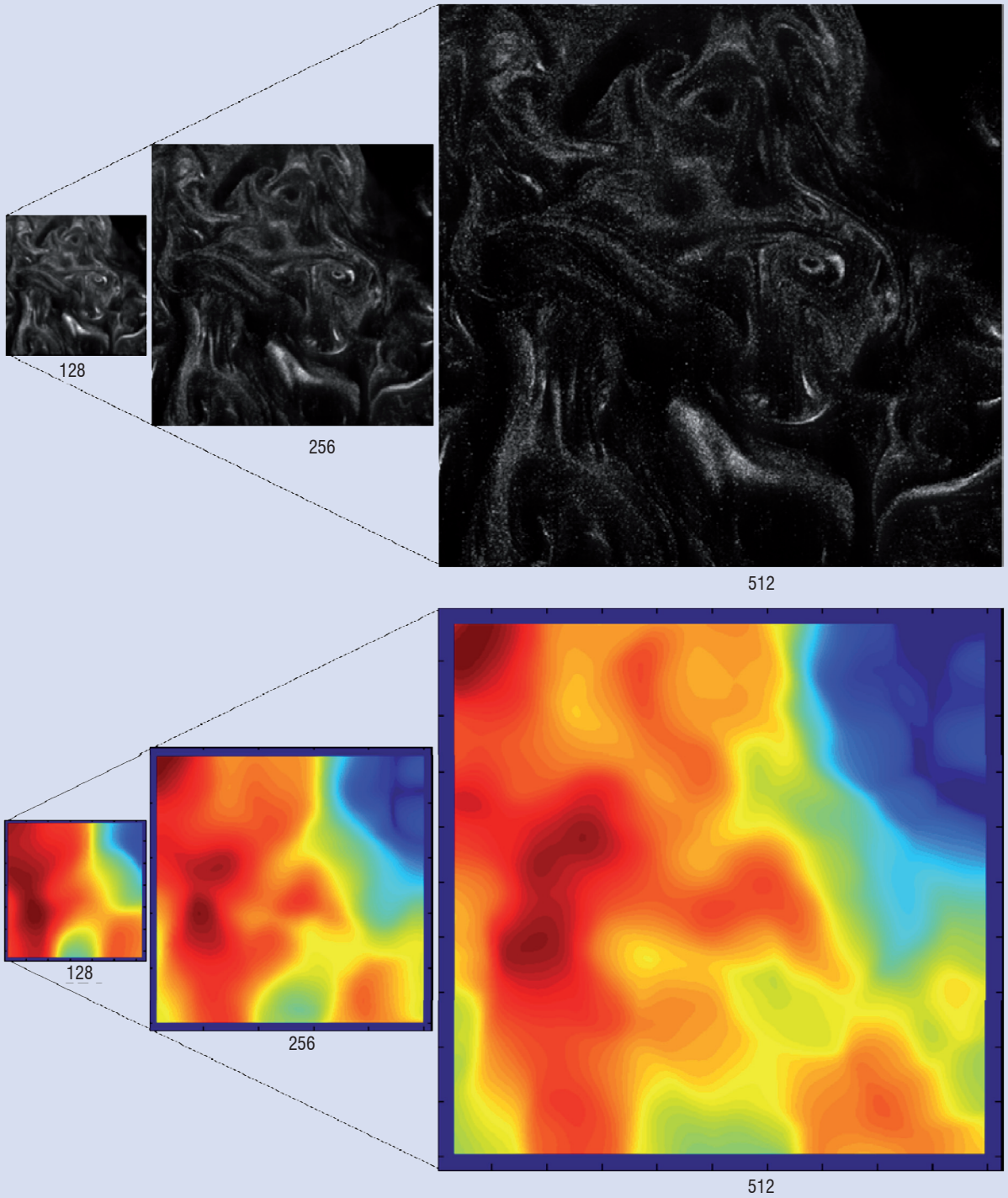

Figure B4 - 02. Three steps of a multi-resolution coarse-to-fine estimation on 2 images of the dataset “Package3” from the FLUID project [5]. Top: image pyramid, from left to right, level 3, 2, 1). Bottom: estimated displacement field norm, window-based FOLKI method with Gaussian weight function of standard deviation 12. From left to right, intermediate results at level 3 (norm max = 2) , 2 (norm max = 4), 1 (norm max = 8).

Efficient solvers for the internal linearized problem

As already mentioned, at each iteration of the optimization, an internal linearized problem has to be solved, with a very large Hessian matrix made of blocks with a diagonal band structure defined by the chosen regularizing functional. Most regularizing functionals imply low-order derivatives and lead to short-range interactions between pixels. For instance, using the Horn and Schunck functional (2) and a quadratic regularization, the stationary equations for the 1D case take the following form:

$$ad_k + b + \frac{d_{k-1} - 2d_k + d_{k+1}}{2h} = 0 \quad \forall k \tag{6}$$

In 2D this model only involves the 4-nearest neighbors of each pixel. The Gauss-Seidel (GS) algorithm (and variants like Jacobi or SOR techniques) is a simple and popular solver for these problems. GS is essentially a pixelwise updating scheme: for each pixel, the displacement d_k is updated by solving (6) with all other displacements $d_l, l \neq k$ fixed. The whole algorithm repeats several sweeps on the image.

The GS algorithm is considered to be an efficient smoother. In $Ad = b$ linear problems, with local dependencies such as (6), GS is very efficient at reducing the high frequency part of the error – in other terms, if d^* denotes the exact solution, d_0 an initial estimate and d_1 the output of a GS iteration, $d_1 - d^*$ has a lower frequency content than $d_0 - d^*$, i.e., it is smoother. Conversely, short-range dependencies mean that GS is very slow in propagating the low-frequency components of the solution. A large number of sweeps are required to achieve a correct convergence.

The logic of multigrid (MG) [19] methods is to use a smoother such as GS but at coarser scales. Indeed, working at coarse scale accelerates the propagation of low-frequency characteristics by GS. Moreover, as problem dimensions are reduced at coarse scales, running the GS algorithm is also cheaper. Therefore, MG methods are theoretically the most efficient techniques for elliptical PDE.

Multigrid methods should not be confused with the multi-resolution estimation process. Multi-resolution estimation deals with the non linearity of the registration criterion with a coarse-to-fine strategy. Multigrid methods are used to speed up the resolution of the linearized sub-problems and use various cycles on the resolution levels (or scales), not only coarse-to-fine: see Box 5.

MG methods are becoming the new standard of fast variational optical flow computation, providing gain factors higher than 20 when compared to classical GS-like algorithms for real-time (i.e. 60 Hz) processing, as been reported on small images (120 x 160 pixels) in [7].

Conclusion

This paper reports the work on fluid dynamics estimation and visualization conducted in the Onera's project MEMFIS. Window correlation methods, popular in the PIV community, have been reviewed, together with the regularization framework (also called variational approach) usually adopted in computer vision. In the line of [3], a unified framework merging the two approaches in a compound criterion has been proposed. But the main subject has been to describe recent algorithmic developments, such as fast iterative correlation techniques, which are at the heart of the window-based FOLKI algorithm [12], and multi-resolution/multigrid optimization schemes. Combined with a GPU implementation, these approaches can already process PIV data at video rate, based on a simple window correlation paradigm. In the near future, there is no doubt that real-time performance will be also achievable using more sophisticated techniques, based on physically-sound models.

These new algorithmic solutions could be the basic engine of a video rate velocity field visualization and interpretation toolbox. They will provide real time computing of the velocity fields inside the visualization tool, so that neither pre-computing nor storing of displacement fields will be necessary. Thus, based on PIV images alone, the user will be able to visualize the salient phenomena while browsing the PIV image sequence, in order to select a spatiotemporal zone and suitable processing in real-time, like, for instance, the detection and tracking of a vortex.

Such combination of recent data processing solutions open the way to a major development in fluid dynamics studies of experimental data. Indeed, the profound changes that we have reported in terms of data processing takes place in a context of great changes both on the experimental side, with new acquisition settings (Time Resolved PIV, tomographic PIV, etc.) and on the numerical side, where finer simulation tools have become available. We think that there is a major opportunity for advanced data processing techniques, based on physical regularization and variational approaches, to realize a smart interface between both sides. We have tried to show that several recent results concerning algorithmic and architectural problems provide solutions to meet this challenge in the near future. In our view, the next step is to launch multidisciplinary studies between experimentalists, physicists and data processing specialists to develop innovative interpretation tools ■

Box 5 - Multigrid schemes

MG methods are used to speed up the resolution of a linear system such as $Ad = b$ based on a smoother like Gauss-Seidel (GS). Let d^* be the true solution of the system, d_0 the current solution and $e_0 = d_0 - d^*$ the current error. As mentioned in the text, a few sweeps of the GS algorithm starting from d_0, an operation that we denote by GS(A, b, d_0), leads to another estimate d_1 and reduces the high-frequency part of the error, i.e. the resulting error $e_1 = d_1 - d^*$ is smoother than e_0.

MG methods consist of solving the problem on coarse grids using few iterations of a smoother (here Gauss-Seidel or SOR) and to correct back d_0 on the finest grid. Two things are then required: a reduction operator $\mathcal{R}$ that projects the smoothed error e_0 and the linear system (A,b) to a coarser level and a prolongator $\mathcal{P}$ that interpolates the correction at some coarse level to the finer level. The interpolation in $\mathcal{P}$ will generally introduce high frequency errors in the solution: this error is reduced by smoothing again (post-smoothing) using GS.

The simplest "two grids" scheme algorithm is:

- Get a first solution on the fine grid GS$(A, b, 0) \rightarrow d_0$
- Compute residual: $r_0 = b - Ad_0$
- Error approximation on coarse grid (reduction/smoothing) : GS$(\mathcal{R}A, \mathcal{R}r_0, \mathcal{R}0) \rightarrow e_1$
- Correction of the current solution: $d = d_0 + \mathcal{P}e_1$
- Smooth the corrected solution: GS$(A, b, d) \rightarrow d_1$

This procedure can be generalized to more than two grids by recursion on the error e, and there are several MG "cycles", such as the V and W-cycles (see Figure B5 - 01).

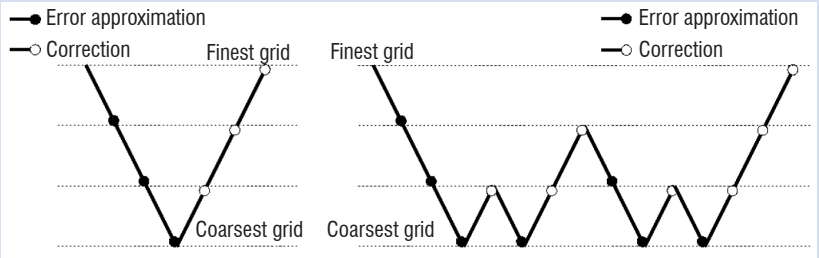

Figure B5 - 01 - Multigrid methods. V-cycle (left) and W-cycles (see text).

In the "full multigrid" scheme, sketched in Figure B5 - 02, we start the algorithm on the coarsest grid with some iteration of the chosen smoother GS (we can also perform a direct resolution because at this scale, the linear system is of small and its resolution is cheap). This approximation is used as an initialization for a multigrid W-cycle (or V-cycle) starting from the next finer grid. But we also merge this process into a multi-resolution estimation process, as explained: the prolongated displacement field is used to change the current registration problem and update the linearized system. Recursively, every solution found on a coarse grid is used for initialization/relinearization by prolongation for the solver on the next finer grid. We can also perform multiple consecutive multigrid cycles on the same resolution to get a better approximation.

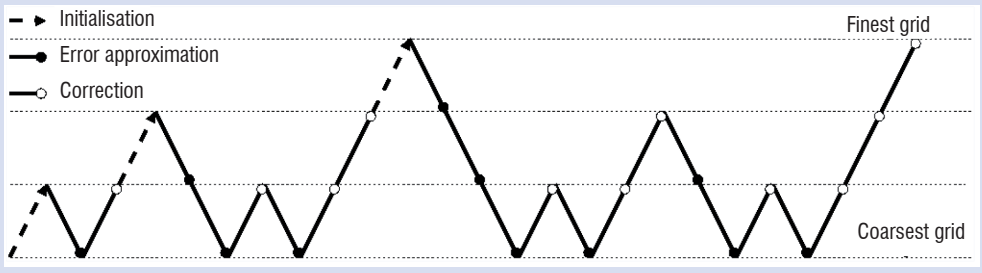

Figure B5 - 02 Full multigrid method. The basic scheme is a W-cycle, which is merged into a coarse-to-fine multi-resolution process.

References

[1] B. HORN, B. SCHUNCK - *Determining Optical Flow,* Technical Report, Massachusetts Institute of Technology, April 1980.

[2] B. LUCAS, T. KANADE - *An iterative Image Registration Technique with an Application to Stereo Vision*. Proceedings DARPA Image Understanding Workshop, pp. 121-130, April 1981.

[3] A. BRUHN, J. WEICKERT - *Lucas/Kanade Meets Horn/Schunck: Combining Local and Global Optic Flow Methods*. International Journal of Computer Vision, vol. 61, n° 3 pp. 211-231, 2005.

[4] P. RUHNAU, T. KOHLBERGER, C. SCHNÖRR, H. NOBACH - *Variational Optical Flow Estimation for Particle Image Velocimetry.* In Experiments in Fluids, vol. 38, pp. 21-32, 2005.

[5] *Interdisciplinary Projet FLUID (FLUid Image analysis and Description)* website http://fluid.irisa.fr/ (data used in the illustrations: http://fluid.irisa.fr/Data/Package3LaVision/), 2006.

[6] J. IDIER (Ed.) - *Bayesian Approach to Inverse problems*. Coll. Digital Signal and Image Porcessing, ISTE – Wiley, London, 2008.

[7] A. BRUHN, J. WEICKERT, T. KOHLBERGER, C. SCHNÖRR - *A Multigrid Platform for Real-Time Motion Computation with Discontinuity-Preserving Variational Methods.* in International Journal of Computer Vision, vol 70, n °3 pp. 257-277, 2006.

[8] T. CORPETTI, E. MÉMIN, P. PÉREZ - *Dense Estimation of Fluid Flows*. IEEE on Pattern Analysis and Machine Intelligence, vol 24, n° 3, march 2002.

[9] P. RUHNAU, C. SCHNÖRR - *Optical Stokes Flow Estimation: An Imaging-Based Control Approach.* in Experiments in Fluids, vol. 42, pp. 61-78, 2007

[10] P. RUHNAU, A. STAHL, C. SCHNÖRR - *Variational Estimation of Experimental Fluid Flows with Physics-based Spatio-temporal Regularization*. Measurement Science and Technology, vol. 18, pp. 755-763, 2007.

[11] S. BAKER, I. MATTHEWS - *Lucas-Kanade 20 years on: A unifying framework*. International Journal of Computer Vision, vol. 56, n° 3, pp. 221–255, 2004.

[12] G. LE BESNERAIS, F. CHAMPAGNAT - *Dense Optical Flow by Iterative Local Window Registration.* ICIP 2005. IEEE International Conference on Image Processing, pp. 137-140, vol. I, 2005.

[13] M. RAFFEL, C. WILLERT, J. KOMPENHANS - *Particle Image Velocimetry: A Practical Guide*. Springer-Verlag, Berlin Heidelberg, 1998.

[14] A. K. PRASAD - *Stereoscopic particle image velocimetry.* Experiments in Fluids, vol. 29, pp. 103-116, 2000.

[15]B. LECLAIRE, B. JAUBERT, F. CHAMPAGNAT, G. LE BESNERAIS, Y. LE SANT - *FOLKI-3C: a Simple, Fast and Direct Algorithm for Stereo PIV.* Proc. 8th Symposium on Particle Image Velocimetry, PIV'09, Melbourne, Victoria, Australia, August 25-28, 2009.

[16] T. LINDEBERG - *Scale-space theory in computer vision*. Kluwer Academic Publishers, 1994.

[17] P. BURT, T. ADELSON - *The Laplacian Pyramid as a Compact Image Code*. IEEE Trans. Communications, vol. 9, n°4, pp. 532–540, 1983.

[18] M. LEFÉBURE, L.D. COHEN - *Image Registration. Optical Flow and Local Rigidity*. Journal of Mathematical Imaging and Vision, vol 14, pp. 131-147, 2001.

[19] P. WESSELING - *An introduction to multigrid methods*. John Wiley and sons, 1991.

[20] F. CHAMPAGNAT, A. PLYER, G. LE BESNERAIS, B. LECLAIRE AND Y. LE SANT - *How to compute dense PIV vector fields at video rate?* Proc. 8th Symposium on Particle Image Velocimetry, PIV'09, Melbourne, Victoria, Australia, August 25-28, 2009.

[21] C. BROSSARD, J.-C. MONNIER, P. BARRICAU, F.-XAVIER VANDERNOOT, Y. LE SANT, F. CHAMPAGNAT, G. LE BESNERAIS - *Principles and Applications of Particle Image Velocimetry.* Aerospace Lab n° 1, December 2009.

[22] T. CORPETTI, P. HÉAS, E. MÉMIN, AND N. PAPADAKIS - *Pressure image assimilation for atmospheric motion estimation*. Rapport de recherche INRIA/RR6507, 2008.

[23]G. LE BESNERAIS, F. CHAMPAGNAT - *B-Spline Image Model for Energy Minimization-Based Optical Flow Estimation*. IEEE Trans. on Image Processing, vol. 15, n° 10, pp. 3201-3206, oct. 2006.

[24]T. CORPETTI, D. HEITZ, G. ARROYO, E. MÉMIN, A. SANTA-CRUZ - *Fluid Experimental Flow Estimation Based on an Optical-Flow Scheme*. Experiments in Fluids, vol 40, n° 1, pp. 80-97, jan. 2006.

[25] G. M. QUÉNOT, J. PAKLEZA, T. A. KOWALEWSKI - *Particle image velocimetry with optical flow*. Experiments in Fluids, vol. 25, pp. 177-189, 1998.

Acronyms

GPU (Graphical Processing Unit)
PSP (Pressure Sensitive Paint)
MDM (Model Deformation Measurement)
PIV (Particle Image Velocimetry)
IW (Interrogation Window)
OFC (Optical Flow Constraint)
MG (Multi Grid)

AUTHORS

Guy Le Besnerais graduated from the Ecole Nationale Supérieure de Techniques Avancées in 1989 and received a Ph.D. degree in physics from the Université de Paris-Sud, Orsay, France, in 1993. He joined Onera in 1994, where he is now a senior scientist in the Modeling and Information Processing Department. His work concerns inversion problems in imagery and computer vision, with an emphasis on embedded perception for autonomous aerial robots.

Frédéric Champagnat graduated from the Ecole Nationale Supérieure de Techniques Avancées in 1989 and received a Ph.D. degree in physics from the Université de Paris-Sud, Orsay, France, in 1993. From 1994 to 1995, he held a Postdoctoral position with the Biomedical Engineering Institute, Ecole Polytechnique, Montreal, QC, Canada. Since 1998, he has been with the Onera, Chatillon, France. His main interests are in the field of spatio-temporal processing for space or aerial image sequences, in particular registration, motion estimation, super-resolution, and detection.

Aurelien Plyer has been a Onera-Laga PhD student since 2008. He received his Master of Science in Computer Science from Universite Pierre et Marie Curie (Paris 6) in 2008. His research deals with video analysis and interpretation of aerial videos within a urban context. He uses GPU programming in order to implement real-time processing.

Benjamin Leclaire graduated from the Ecole Polytechnique in 2001 and received his Ph.D. degree from the same university in 2006. During his Ph.D., he worked on the dynamics of turbulent rotating flows in the Fundamental and Experimental Aerodynamics Department of Onera. He now holds a position of research scientist in this department. His activity includes industrial wind-tunnel tests and fundamental research on vortex breakdown and PIV (Particle Image Velocimetry). In this latter field, his interests are focused more specifically on motion detection and flow characterization.

Riadh Fezzani holds a Masters in mathematical modeling and computational methods from the University Paul Sabatier (Toulouse 3) and is currently preparing a PhD thesis in the French Aerospace Lab (Onera).

Yves Le Sant Researcher at Onera since 1983. His first studies concerned wall interferences and the development of an adaptive test section. Then he was involved in applying and developing many measurements methods, such as heat flux assessment, temperature and pressure sensitive paints and model deformation. His current activities are in the field of image processing applications, such as in Particle Image Velocimetry.